Photocurrent spectra of bilayers and blends of the organic donor-acceptor system CuPc/C_{60}

Thomas Stübinger and Wolfgang Brütting

University of Bayreuth, Experimental Physics II, 95440 Bayreuth, Germany

ABSTRACT

Photocurrent spectra and quantum efficiency are investigated in photovoltaic cells with the electron donor material Cu−phthalocyanine (CuPc) together with C_{60} as electron acceptor material. By a systematic variation of both layer thicknesses in bilayer devices with the main process of photocurrent generation at the donor-acceptor interface we found a significant influence on photocurrent generation due to optical interference effects and determined the optimum layer thicknesses for both materials. The effective dissociation interface is increased by introducing a 1 : 1 blend of both materials between the pure CuPc and C_{60} layers. The more extended active volume of exciton dissociation leads to higher quantum efficiencies (IPCE up to $\approx 22\%$) of the photovoltaic effect in comparison to the heterojunction bilayer devices.

Keywords: Organic Solar Cells, Photovoltaic Cells, Fullerenes, Phthalocyanines, Photocurrent Spectra

1. INTRODUCTION

Organic photovoltaic devices based on conjugated polymers and low molecular-weight materials with high absorption coefficients are promising candidates for efficient photon-to-current conversion.[1–9] While photovoltaic cells consisting of a single organic layer in general exhibit low efficiency of energy conversion,[4,5] blends[6,10] and heterojunctions[1,3,11] of materials with high electron affinity considerably enhance the incident photon-to-current efficiency (IPCE) but also the more important power conversion efficiency η_P.

The primary step of photocurrent generation in organic photovoltaic devices is the creation of strongly bound excitons after light absorption in the active absorbing parts of the devices with exciton binding energies E_B of some tenths of an eV (e.g. $E_B = 0.6$ eV for excitons in CuPc).[12] The generation of separated charges occurs as a result of exciton dissociation by interaction with interfaces, impurities or defects, or in high electric fields. Competing pathways are radiative and nonradiative recombination, the former being important especially in materials with high photoluminescence efficiency. A very efficient exciton dissociation process has been found by Sariciftci et al.[13] in the ultrafast photoinduced electron transfer from photo-excited conjugated polymers to the lowest unoccupied molecular orbital (LUMO) of the Buckminsterfullerene C_{60}. This electron transfer takes place on a subpicosecond timescale,[13,14] which is about three orders of magnitude faster than typical radiative lifetimes of a few nanoseconds. Therefore the main dissociation process in heterojunction cells takes place only in the immediate vicinity of the donor-acceptor interface. Dissociation processes in the bulk region of the materials can be neglected. In contrast, the actual dissociation interface is substantially increased in donor-acceptor blend systems with an active volume of exciton dissociation in the whole blend system. Therefore one can expect that the efficiency of charge carrier generation is substantially higher in blend systems in comparison to bilayer devices with the same total layer thickness. It will then mainly depend on the electrical transport properties of the specific layers whether the values of IPCE and η_P can be increased, too.

The generation of excitons is strongly dependent on the distribution of the light intensity inside the absorbing material, which consequently influences the photovoltaic properties of the cells.[11] Additionally, reflections at the metal/organic interface leading to optical interference can significantly affect the distribution of the light intensity inside the device. These effects become especially important for thin film structures, where layer thicknesses are comparable to the penetration depth of the incident light, and also in the case of a highly reflecting rear contact as, for example, in the case of the metal electrodes normally used in organic photovoltaic cells. Especially in bilayer

Further author information: (Send correspondence to Thomas Stübinger)
E-mail: Thomas.Stuebinger@uni-bayreuth.de

devices with a clearly defined position of the dissociation interface the layer thicknesses of both the donor and the acceptor layer are important parameters, which influence the quantum efficiencies of the cells.

In this paper we report on experimental results concerning the influence of the organic layer thicknesses on short-circuit photocurrent spectra of thin film organic photovoltaic devices. In particular we focus on possible optical interference effects due to reflecting electrodes and on the influence of an increased active volume of exciton dissociation in blend systems on photocurrent generation. We used donor-acceptor bilayer systems and blend systems of the low molecular-weight materials Cu−phthalocyanine (CuPc) and Buckminsterfullerene C_{60}.

2. EXPERIMENTAL

2.1. Device Fabrication and Characterization

The used materials are schematically shown in Fig. 1. In the case of the bilayer devices the donor-acceptor system CuPc/C_{60} was sandwiched between a transparent, conducting anode (indium tin oxide, ITO), through which the cell was illuminated, and an opaque (reflecting) Al counterelectrode. We used commercially available glass substrates coated with ITO (Merck-Balzers, Flachglas), which were cleaned with different solvents in an ultrasonic bath followed by an oxygen plasma-treatment in order to enhance the work function of ITO.

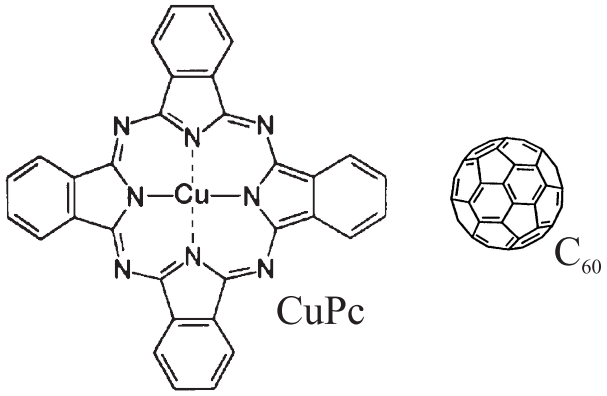

Figure 1. Chemical structure of Cu−phthalocyanine (CuPc) and Buckminsterfullerene C_{60}.

The CuPc/C_{60} donor-acceptor systems were fabricated by evaporation of both the CuPc and the C_{60} layer under high vacuum conditions ($< 1 \times 10^{-6}$ mbar) with a mean evaporation rate of ≈ 0.1 nm/s. Systematic variation of the layer thicknesses was performed by preparing up to six devices with different thickness in only one vacuum-cycle in order to obtain the same preparation conditions for comparable investigations. Detailed information about the different layer thicknesses used in these bilayer devices can be obtained from Fig. 4.

In the case of the blend systems the different device structures are schematically shown in Fig. 2. The CuPc:C_{60} blends, sandwiched between a CuPc layer and a C_{60} layer, were achieved by co-evaporation of the two materials in a vacuum chamber with effusion cells for organic materials in a vacuum of 5×10^{-8} mbar. With slightly different evaporation rates in the order of 0.02 nm/s a mixing ratio of $\approx 1:1$ was obtained. The layer thickness of the blend was increased systematically in steps of 20 nm (see Fig. 2, devices $(2-4)$), keeping the total layer thickness at a fixed value of 80 nm. We also prepared CuPc:C_{60} blends directly sandwiched between ITO and Al, however they appeared to be not very useful for photoelectric characterization because of a very low signal-to-noise ratio and high leakage currents, so we did not take them into further consideration.

After evaporation of the organic layers in all the different systems the metal cathode (aluminum) was evaporated under high vacuum conditions. By a shadow mask four independent contacts each with an area of ≈ 14 mm^2 were obtained on one substrate. In order to minimize aging effects (e.g. by oxygen or moisture), devices were stored inside a glove-box system under nitrogen atmosphere after preparation and between measurements.

For the photocurrent spectroscopy a 150 W xenon arc lamp served as a source of white light. This white light passed through a Bentham monochromator in order to obtain monochromatic light which was then focused onto the

entrance window of the cryostat. In our experiments, we used a blazed grating in the monochromator, ruled with 1200 lines/mm, together with appropriate long-pass filters to cover the whole visible spectral range ($380 - 780$ nm). Measurements of short-circuit photocurrents of the different devices were performed with a Keithley 6517 electrometer during illumination with monochromatic light through the transparent ITO-anode. The intensity of the light was measured separately using a calibrated silicon photodiode placed at the same position as the samples. For the current-voltage (I-V) characteristics under white light illumination (with a halogen lamp) we used a Keithley 236 source-measure unit. All photoelectric measurements were performed at room temperature under high vacuum conditions to prevent the devices from photo-oxidation. Optical absorption spectra were measured on films deposited on quartz glass substrates with a Perkin Elmer Lambda2 UV/VIS-Spectrometer.

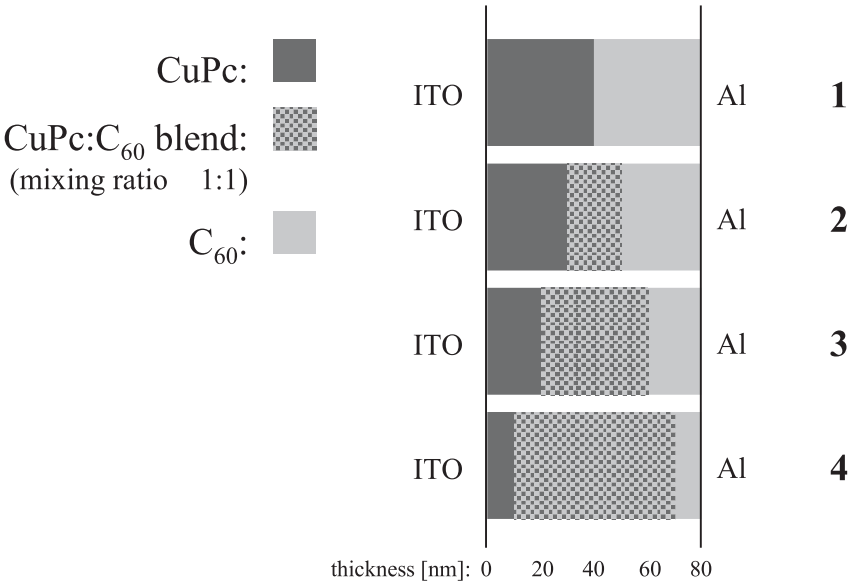

Figure 2. Device structures with corresponding layer thicknesses: (1) CuPc/C_{60} bilayer structure and $(2-4)$ blend systems CuPc:C_{60} (mixing ratio $\approx 1:1$) sandwiched between layers of CuPc and C_{60}.

Before correcting for the wavelength-dependent illumination intensity we verified that there was a linear dependence of the photocurrent on the intensity of the incident light ($J_{\mathrm{Photo}} \propto {I_0}^{\tau}$) for all our studied devices with $\tau = 1$. The light intensity dependence of the photocurrent as described by the value of the exponent τ is related to the efficiency of exciton generation and dissociation and the electrical characteristics of the photovoltaic cell. With $\tau = 1$ bimolecular recombination can be neglected and therefore all photocurrent spectra could easily be normalized to a constant light intensity for monochromatic illumination (in our case: 140 μW/cm^2).

2.2. Optical Absorption Spectra

The absorption spectra of the two organic materials are shown in Fig. 3(a). CuPc and C_{60} have almost non-overlapping but complementary absorption spectra in the whole visible spectral range. In bilayer devices we can therefore distinguish between light absorption in the CuPc layer and in the C_{60} layer by choosing the adequate wavelength. This allows to investigate separately effects like exciton generation and diffusion in the absorbing material or optical interference.[15]

In the blend systems the optical absorption spectra are shown in Fig. 3(b) (Numbers $(1-4)$ correspond to the device structures as shown in Fig. 2). The total layer thickness of the devices was kept fixed to 80 nm and the ratio of CuPc:C_{60} is the same in all devices. Therefore differences in the optical absorption spectra, especially in the range of C_{60} absorption $(400 - 550$ nm) and of CuPc absorption $(550 - 750$ nm), result from different distributions of the organic materials and from different positions of the interfaces in the devices. The total layer thickness is much smaller than the wavelength of incident light, so different coherence phenomena occur, which in contact with highly

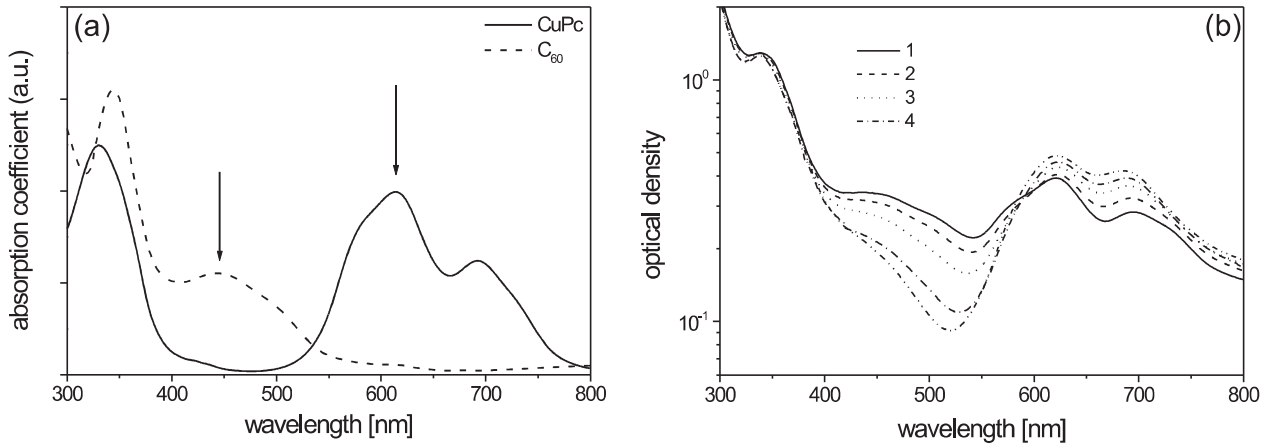

Figure 3. (a) Absorption spectra of Cu−phthalocyanine (CuPc) and Buckminsterfullerene C_{60} in solid thin films. CuPc and C_{60} show complementary absorption spectra in the visible spectral range. (b) Optical density spectra of the blend systems CuPc:C_{60} (Numbers $(1-4)$ correspond to the device structures shown in Fig. 2).

reflecting electrodes lead to optical interference effects (discussed in detail in subsection 3.2 for CuPc/C_{60} bilayer devices). Only in the UV range ($\lambda < 380$ nm), where the absorption of both CuPc and C_{60} is high, coherence phenomena are less dominant and the optical density is the same in all cases. Therefore spectrally and spatially dependent absorbance in the whole device, respectively coherence effects, cannot be neglected in discussing light absorption and exciton generation in these systems.

3. RESULTS AND DISCUSSION

For organic single layer photovoltaic devices, the relationship between photocurrent and absorption spectra can be classified into two types: symbatic and antibatic response.[16] In the former case the photocurrent spectrum correlates well with the absorption spectrum, so that the maximum photocurrent is obtained at the wavelength of the strongest absorption. In the latter case, there is a local minimum of the photocurrent at maximum absorption and the maxima of the photocurrent spectrum occur for photon energies near the absorption edge. In single layer devices with one Ohmic and one Schottky contact antibatic behaviour typically occurs for illumination through the Ohmic contact and symbatic response for illumination through the Schottky contact.[17,16] In this case the main exciton dissociation takes place at the Schottky contact due to the high internal electric field in the vicinity of the electrode. A transition from symbatic to antibatic behaviour can be observed by increasing the layer thickness of the organic semiconductor material from very thin layers comparable to the penetration depth ($d \lesssim (\alpha_{max})^{-1}$) to very thick layers ($d \gg (\alpha_{max})^{-1}$) resulting in thickness-dependent photocurrent spectra.

3.1. Thickness-Dependence of Photocurrent Spectra in Bilayer Devices

We investigated different CuPc/C_{60} bilayer systems varying systematically the thicknesses of the two layers.

The additional fullerene layer does not influence the distance between the illuminated ITO-electrode and the position of the dissociation interface CuPc/C_{60} but improves the photon-to-electron conversion efficiency as compared to the respective CuPc single layer devices with the same donor layer thicknesses.

Let us first discuss the variation of the CuPc layer thickness for a fixed C_{60} layer thickness. There are two main contributions to the photocurrent in the CuPc/C_{60} bilayer system as can be seen in Fig. 4(a). The first one in the long wavelength range $(550-780$ nm) is due to absorption in the CuPc layer. A second contribution to the photocurrent spectra is found in the wavelength range of negligible CuPc absorption between 400 nm and 500 nm. In this range the C_{60} absorption is high and exciton generation occurs in the bulk of C_{60}. In order to achieve such a significant photocurrent contribution an efficient dissociation mechanism at the donor-acceptor interface is required.

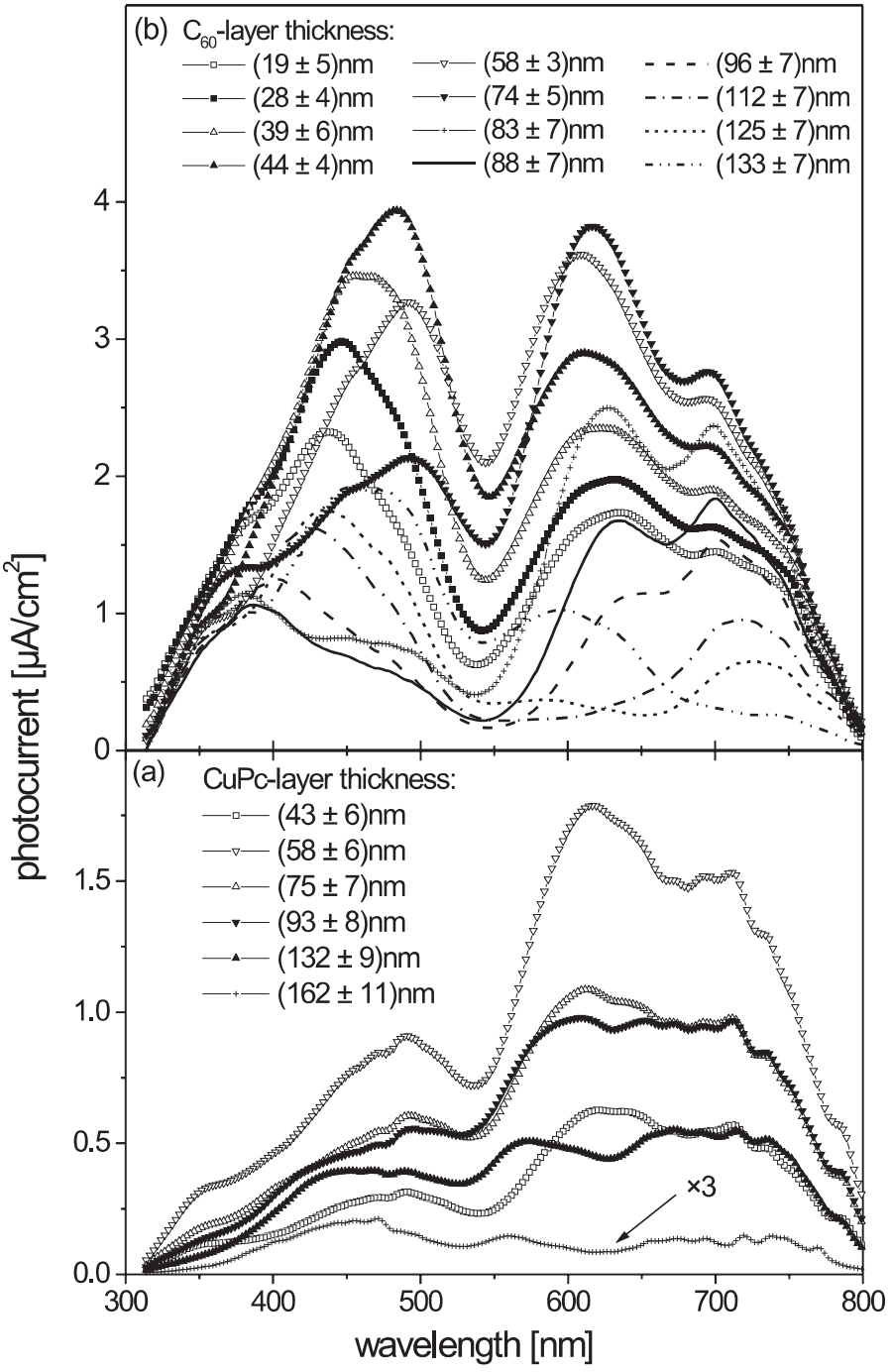

Figure 4. Photocurrent spectra of ITO/CuPc/C_{60}/Al bilayer devices. (a) Variation of the CuPc layer thickness at a fixed C_{60} layer thickness of (38 ± 4) nm and (b) variation of the C_{60} layer thickness at a fixed CuPc layer thickness of (57 ± 4) nm.

This can be achieved by a hole transfer from generated excitons in C_{60} to the highest occupied molecular orbital (HOMO) of CuPc. There is also the typical transition from symbatic to antibatic response of the photocurrent spectra with increasing CuPc layer thickness in the long wavelength range ($550 - 780$ nm), the region of bare CuPc absorption. For thin CuPc layers ($d < 80$ nm) the photocurrent maximum occurs at the wavelength of the absorption peak. At thicker CuPc layers this photocurrent maximum turns into a local minimum representing the antibatic response. Further there is a global maximum of the photocurrent for a CuPc layer thickness of (58 ± 6) nm. In the wavelength region of bare C_{60} absorption there is no significant change of the shape of the photocurrent contribution with increasing CuPc layer thickness.

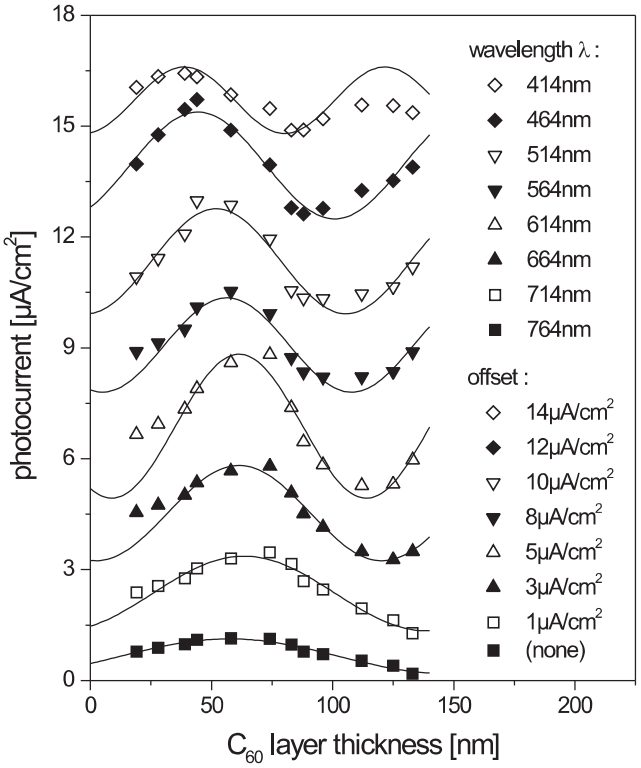

Figure 5. Dependence of the photocurrent on the C_{60} layer thickness for different wavelengths in ITO/CuPc/C_{60}/Al bilayer devices. Data are taken from Fig. 4(b). The lines are fit curves using Eq. (1) (see subsection 3.2).

Through the variation of the C_{60} layer thickness from (19 ± 5) nm to (133 ± 7) nm at a constant CuPc donor layer thickness of (57 ± 4) nm we obtained significant changes of the photocurrent spectra in the whole visible spectral range (see Fig. 4(b)). In the range of CuPc absorption ($550 - 780$ nm) the photocurrent first increases with increasing C_{60} layer thickness, then reaches a maximum photocurrent at the wavelength of the absorption peak for a C_{60} layer thickness of (74 ± 5) nm and afterwards decreases with further increase of the C_{60} layer thickness until it starts to increase again around 600 nm for the thickest C_{60} layer. Because of the constant CuPc layer thickness no transition from symbatic to antibatic response is visible. At shorter wavelengths ($400 - 500$ nm) there is an equivalent behaviour, but the global maximum is already reached at a thinner C_{60} thickness of (44 ± 4) nm. This means that the optimum C_{60} layer thickness is dependent on the wavelength of the incident monochromatic light. There is also a continuous red-shift of the photocurrent peak in the short wavelength range, which is repeating periodically with increasing C_{60} layer thickness. These changes of the shape and magnitude of the photocurrent spectra indicate an optical interference effect in these bilayer devices at the dissociation interface leading to periodically modulated photocurrent spectra, which will be discussed in the following subsection.

3.2. Interference Effect

In order to prove the occurrence of the optical interference effect at the dissociation interface, the obtained photocurrents of the bilayer devices are plotted versus the C_{60} layer thickness for different wavelengths in Fig. 5. A periodic modulation of the photocurrent as a function of the C_{60} layer thickness with increasing period for larger wavelengths can be seen. The lines in Fig. 5 are fit curves using a simple interference model (neglecting C_{60} absorption) which will be discussed below.

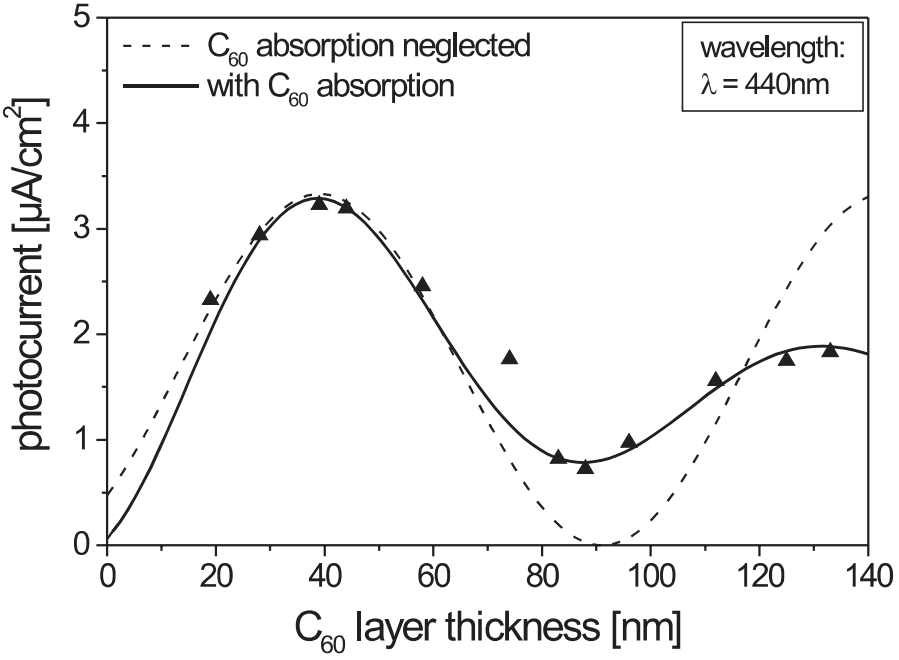

Figure 6. Interference effect in the ITO/CuPc/C_{60}/Al bilayer device: comparison of measured data with the interference model once including and once neglecting additional C_{60} contribution.

The light intensity at the dissociation interface is strongly influenced by optical interference effects due to the reflecting Al back-contact, which is the most dominant boundary condition. By increasing the C_{60} layer thickness d also the distance between the back-reflecting Al-electrode and the dissociation interface is changed leading to a periodic modulation of the light intensity inside the device. The light intensity $I_1(d, \lambda)$ at the donor-acceptor interface is given by the following equation (only light propagation perpendicular to the substrate plane is considered):

$$I_1(d, \lambda) = I_0(\lambda) \sin^2 [k(\lambda)d - \varphi(\lambda)] \quad \text{with} \quad k(\lambda) = \frac{2\pi n(\lambda)}{\lambda} \tag{1}$$

Therein $I_0(\lambda)$ is the intensity of incident monochromatic light (after passing the CuPc layer), $k(\lambda)$ the wavevector in C_{60}, $n(\lambda)$ the refractive index of C_{60} and $\varphi(\lambda)$ a phase shift.

Equation (1) is only correct if C_{60} absorption is negligible. The additional phase shift $\varphi(\lambda)$ is introduced to allow for a possible shift of the active zone away from the CuPc/C_{60} interface, which can occur when the exciton diffusion length in one of the materials is comparable to the layer thickness. In this case excitons generated far away from the dissociation interface also contribute to the photocurrent leading to a shift of the effective interface position. It has been found that $\varphi \approx 0$ in the wavelength range of C_{60} absorption and $\varphi < 0$ for CuPc absorption, which indicates a relatively large exciton diffusion length in CuPc. On the other hand the possibility of a finite penetration depth of the light waves into the metal electrodes in the range of a few nanometers can also shift the nodes of the standing light waves.

Fits of Eq. (1) to the observed periodic modulation of the photocurrent are shown as lines in Fig. 5. The obtained refractive index of C_{60} is about (2.5 ± 0.3) in the wavelength range $400 - 650$ nm and about (2.0 ± 0.3) above this

range, which is comparable to literature data.[18,11] The drop at about 650 nm can be ascribed to a slight decrease of C_{60} absorption at about the same wavelength (see Fig. 3(a)).

A problem with the simple interference model given by Eq. (1) appears at short wavelengths and for thick C_{60} layers. In the short wavelength range C_{60} absorption is sufficiently high leading to exciton generation in C_{60} and a non-negligible photocurrent contribution as mentioned above. Thus the simple interference model has to be modified by additional terms including absorption $\alpha(\lambda)$ and exciton generation $c(\lambda)$ in the C_{60} layer. The light intensity at the dissociation interface is then given by:

$$I_2(d,\lambda) = I_1(d,\lambda)\exp[-\alpha(\lambda)d] + c(\lambda)[1-\exp(-\alpha(\lambda)d)] \tag{2}$$

The result for the modified model is shown in Fig. 6 for a wavelength of 440 nm (region of strong C_{60} absorption). The exponential decay of the photocurrent due to C_{60} absorption (first term in Eq. (2)) is clearly seen together with an increasing offset of the photocurrent for thicker C_{60} layers (second term in Eq. (2)), which saturates for infinite C_{60} layer thickness at a value of $\approx I_0(\lambda)/4$.

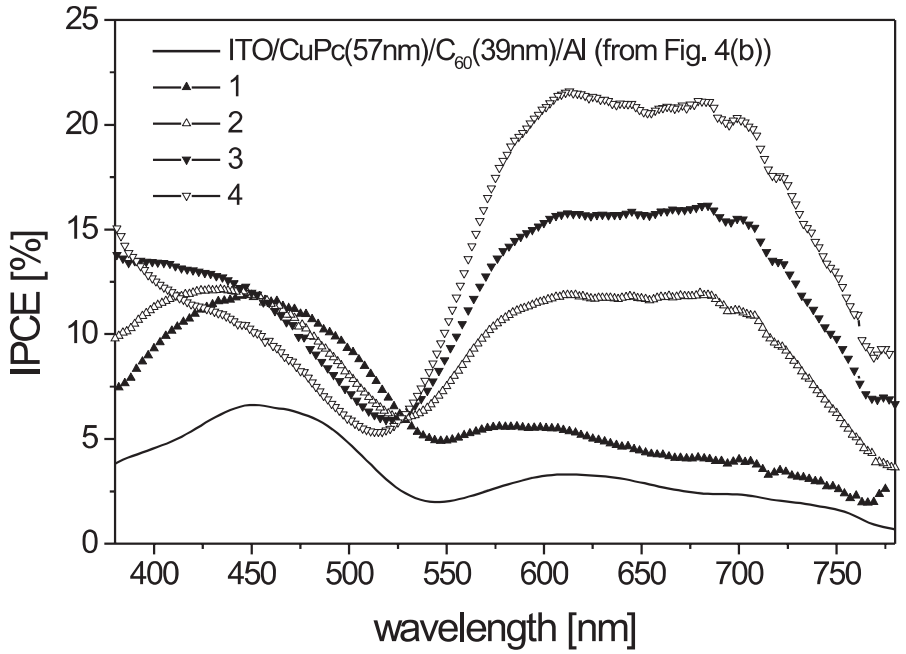

Figure 7. Photocurrent spectra of ITO/CuPc/CuPc:C_{60}($\approx 1:1$)/C_{60}/Al blend systems with variation of the layer thickness of the blend with respect to a fixed total layer thickness between the two electrodes (Numbers $(1-4)$ correspond to the device structures shown in Fig. 2).

As can be seen in Fig. 5 the maximum value of the photocurrent occurs at the first maximum of the periodic modulation with increasing C_{60} layer thickness and is therefore dependent on the wavelength of the incident monochromatic light. By choosing the corresponding thickness the photocurrent efficiency of the device could be maximized under monochromatic light illumination. For the whole visible spectral range and white light illumination, however, the best C_{60} layer thickness must include both main contributions to the photocurrent and should be in the range of $40-60$ nm.

The predicted optimum (35 nm) and worst (80 nm) C_{60} layer thickness calculated for a polymer/C_{60} heterostructure by Pettersson et al.[11] show good agreement with our experimental results at the corresponding wavelength ($\lambda =$ 460 nm, see Fig. 5 and 6). Becker et al.[19] reported that nonradiative energy transfer is important for distances $d \leq (90/n)$ nm from the metal-electrode (n : refractive index). In our case, however, we have found no evidence for exciton quenching due to the Al-metal cathode even for thin C_{60} layers ($d < 40$ nm) since the photocurrent

modulation can be simply described by optical interference. The optimum layer thickness is therefore not influenced by quenching effects of the metal-electrode, at least for the investigated C_{60} layer thicknesses above 20 nm.

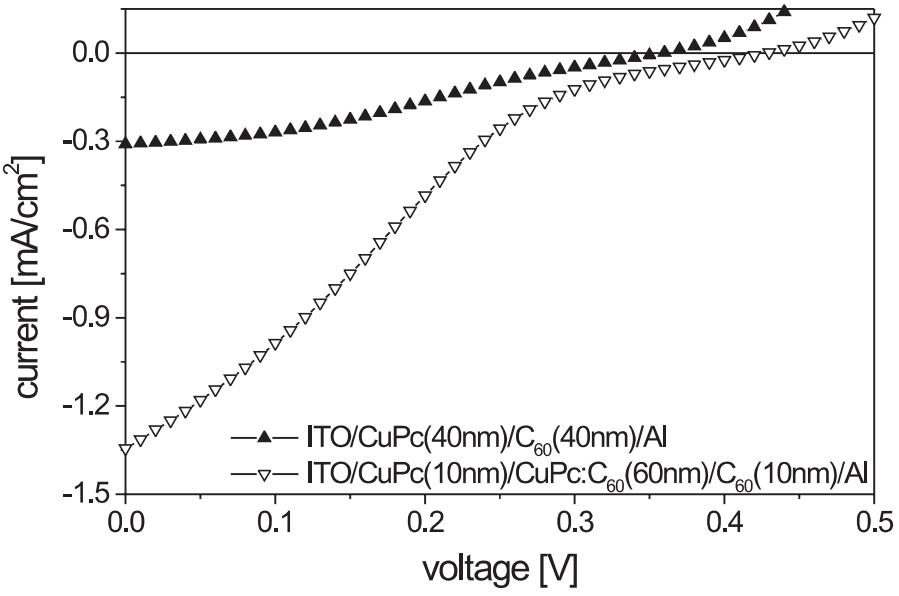

Figure 8. Current-voltage characteristic of a bilayer and a blend system under white light illumination at 40 mW/cm^2.

3.3. Influence of an Additional Blend System

In the above discussed bilayer devices the active zone of exciton dissociation is given by the donor-acceptor interface between CuPc and C_{60}. In the next step we increased this active zone by sandwiching CuPc:C_{60} blends (mixing ratio $\approx 1:1$) between the CuPc and the C_{60} layer and investigated the influence of an effectively increased dissociation interface on the photocurrent spectra. In order to reduce optical interference effects, as described in the previous subsection for bilayer devices, the total layer thickness and the mixing ratio of CuPc and C_{60} was kept fixed in the blend systems. The total layer thickness of 80 nm results from the optimum layer thickness of C_{60} ($40-50$ nm, see Fig. 5) in bilayer devices together with the $1:1$ mixing of the blends.

In devices with an additional layer of the blend system CuPc:C_{60} the spectral photocurrent response changes significantly. As can be seen in Fig. 7 the photocurrent and therefore the quantum efficiency (IPCE) is clearly increased in blend systems. By adding blends with layer thicknesses of 20 nm, 40 nm and 60 nm (corresponding to device number (2), (3) and (4) in Fig. 2) the photocurrent contribution increases continuously in the long wavelength range ($\lambda > 550$ nm). On the other hand there is no significant change of the photocurrent spectra in the short wavelength range between 400 nm and 550 nm. However, the contribution of C_{60} to light absorption in the devices decreases with increasing blend layer thickness as can be seen in the optical absorption spectra (see Fig. 3(b)). This result indicates that electron transport through the devices, especially through the blend and the subsequent C_{60} layer, is not a limiting factor for the photocurrent. For very short wavelengths ($\lambda \approx 350$ nm) there is a change of the photocurrent, which increases with increasing layer thickness of the blend and with decreasing layer thickness of CuPc. Because of strong absorption of both CuPc and C_{60} in this wavelength range, this result indicates that the main contribution comes from exciton generation in C_{60} with a subsequent hole transfer to CuPc. With decreasing distance of the CuPc/blend interface to the ITO-electrode also the efficiency increases. Consequently the hole transport through the blend system and through the CuPc layer seems to be the main limiting factor for all investigated blend systems. A previously discussed bilayer system is also shown in Fig. 7, which corresponds to the photocurrent spectra shown in Fig. 4(b). This bilayer device was prepared in a different vacuum chamber and with different evaporation conditions as described in section 2.1. In comparison the bilayer device prepared with the effusion cells (device (1) in Fig. 2) shows a significant increase of the quantum efficiency in the whole visible spectral range with almost the

same shape of the spectrum. This might be an indicator for an improved morphology of the films and therefore for better electrical transport properties.

The highest IPCE values of 22% in the long wavelength range of CuPc absorption was obtained with an additional blend layer thickness of 60 nm (device (4) in Fig. 2). The increased active volume of exciton generation and dissociation in the additional blend layers lead to more efficient photocurrent generation in the long wavelength range as a consequence of an efficient electron transfer from the excited CuPc to C_{60}.

In addition to the short-circuit photocurrent spectra and the corresponding quantum efficiencies we also investigated current-voltage characteristics under white light illumination. We compared the bilayer (device (1), see Fig. 2) with the blend system (device (4), see Fig. 2) with the thickest blend layer in order to check whether the increased quantum efficiency (IPCE) in the blend system also leads to an enhanced power efficiency η_P. As can be seen in Fig. 8 the additional blend layer between the CuPc layer and the C_{60} layer leads to an increased short-circuit current under white light illumination and the open-circuit voltage changes to a slightly higher voltage ($V_{oc} \approx 0.42$ V) in the blend system. Therefore the power efficiency is also higher in these systems compared to the bilayer devices. With a total intensity of 40 mW/cm^2 for white light illumination a power efficiency $\eta_P \approx 0.3\%$ was obtained. This value is almost one order of magnitude lower than published power efficiencies in conjugated polymer/fullerene blend systems with $\eta_P \approx 2.5\%$.[9] In these systems the transport properties of the separated charge carriers are strongly dependent on the morphology of the blends, which is not fully understood. Furthermore, although the quantum efficiencies in our investigated blend systems are quite high the power efficiency is significantly limited by low filling factors and open circuit voltages, which both linearly contribute to η_P. So, further investigations on optimizing charge transport properties in relation to morphology effects in these systems have to be done.

4. CONCLUSION

We have investigated the influence of layer thickness and optical interference on organic photovoltaic devices in bilayer donor-acceptor heterojunction and blend systems. Assuming that charge carrier separation mainly takes place at the donor-acceptor interface due to a photoinduced electron and hole transfer, we were able to investigate the influence of the specific position of this dissociation interface on the short-circuit photocurrent spectra of CuPc/C_{60} bilayer systems. The advantage of complementary absorption spectra of CuPc and C_{60} allowed us to investigate the interference effect due to standing light waves in the C_{60} layer. From the variation of the C_{60} layer we obtained an optimum thickness of this layer between 40 nm and 60 nm depending on the illumination wavelength. The typical transition from symbatic to antibatic response, leading to the optical filter effect, is obtained by increasing the absorbing CuPc layer thickness. An increased quantum efficiency was achieved in blend systems with a 1 : 1 mixing ratio of CuPc:C_{60} due to an effectively increased active volume of exciton dissociation. With quantum efficiencies of 22% (IPCE) and power efficiencies of $\eta_P \approx 0.3\%$ in these blend systems respectable photovoltaic properties were achieved even without optimization of the corresponding mixing ratio.

ACKNOWLEDGMENTS

Financial support by the Deutsche Forschungsgemeinschaft (Sonderforschungsbereich 481) is gratefully acknowledged.

REFERENCES

1. C. Tang, "Two-layer organic photovoltaic cell," *Appl. Phys. Lett.* **48**, p. 183, 1986.
2. D. Wöhrle and D. Meissner, "Organic solar cells," *Adv. Mater.* **3**, p. 129, 1991.
3. N. Sariciftci, D. Braun, C. Zhang, V. Srdanov, A. Heeger, G. Stucky, and F. Wudl, "Semiconducting polymer-buckminsterfullerene heterojunctions: Diodes, photodiodes, and photovoltaic cells," *Appl. Phys. Lett.* **62**, p. 585, 1993.
4. A. Ghosh and T. Feng, "Merocyanine organic solar cells," *J. Appl. Phys.* **49**, p. 5982, 1978.
5. R. Marks, J. Halls, D. Bradley, R. Friend, and A. Holmes, "The photovoltaic response in poly(p-phenylene vinylene) thin-film devices," *J. Phys.: Condens. Matter* **6**, p. 1379, 1994.
6. G. Yu and A. Heeger, "Charge separation and photovoltaic conversion in polymer composites with internal donor/acceptor heterojunctions," *J. Appl. Phys.* **78**, p. 4510, 1995.

7. J. Schön, C. Kloc, E. Bucher, and B. Batlogg, "Single crystalline pentacene solar cells," *Synth. Met.* **115**, p. 177, 2000.
8. C. Brabec, N. Sariciftci, and J. Hummelen, "Plastic solar cells," *Adv. Funct. Mater.* **11**, p. 15, 2001.
9. S. Shaheen, C. Brabec, N. Sariciftci, F. Padinger, T. Fromherz, and J. Hummelen, "2.5% efficient organic plastic solar cells," *Appl. Phys. Lett.* **78**, p. 841, 2001.
10. J. Rostalski and D. Meissner, "Monochromatic versus solar efficiencies of organic solar cells," *Solar Energy Materials & Solar Cells* **61**, p. 87, 2000.
11. L. Pettersson, L. Roman, and O. Inganäs, "Modeling photocurrent action spectra of photovoltaic devices based on organic thin films," *J. Appl. Phys.* **86**, p. 487, 1999.
12. A. Kahn, "Electronic properties of π-conjugated organic molecular semiconductor interfaces," (Spring Meeting of the German Physical Society, Hamburg), 2001.
13. N. Sariciftci, L. Smilowitz, A. Heeger, and F. Wudl, "Photoinduced electron transfer from a conducting polymer to buckminsterfullerene," *Science* **258**, p. 1474, 1992.
14. B. Kraabel, D. McBranch, N. Sariciftci, D. Moses, and A. Heeger, "Ultrafast spectroscopic studies of photoinduced electron transfer from semiconducting polymers to C_{60}," *Phys. Rev. B* **50**, p. 18543, 1994.
15. T. Stübinger and W. Brütting, "Exciton diffusion and optical interference in organic donor-acceptor photovoltaic cells," *J. Appl. Phys.* **90**, p. 3632, 2001.
16. M. Harrison, J. Grüner, and G. Spencer, "Analysis of the photocurrent action spectra of MEH-PPV polymer photodiodes," *Phys. Rev. B* **55**, p. 7831, 1997.
17. A. Ghosh, D. Morel, T. Feng, R. Shaw, and C. R. Jr., "Photovoltaic and rectification properties of Al/Mg-phthalocyanine/Ag schottky-barrier cells," *J. Appl. Phys.* **45**, p. 230, 1974.
18. M. Kelly, P. Etchegoin, D. Fuchs, W. Krätschmer, and K. Fostiropoulos, "Optical transitions of C_{60} films in the visible and ultraviolet from spectroscopic ellipsometry," *Phys. Rev. B* **46**, p. 4963, 1992.
19. H. Becker, S. Burns, and R. Friend, "Effect of metal films on the photoluminescence and electroluminescence of conjugated polymers," *Phys. Rev. B* **56**, p. 1893, 1997.